Global Change Biology (2008) **14**, 2178–2193, doi: 10.1111/j.1365-2486.2008.01635.x

Evaporation and carbonic anhydrase activity recorded in oxygen isotope signatures of net CO_2 fluxes from a Mediterranean soil

LISA WINGATE*, ULLI SEIBT†, KADMIEL MASEYK‡, JÉRÔME OGÉE§, PEDRO ALMEIDA¶, DAN YAKIR‡, JOAO S. PEREIRA¶ and MAURIZIO MENCUCCINI*

School of GeoSciences, University of Edinburgh, Edinburgh, UK, †Department of Plant Sciences, Cambridge University, Cambridge, UK, ‡Weizmann Institute of Science, Rehovot, Israel, §INRA – Ephyse, Villenave D'Ornon, France, ¶Instituto Superior de Agronomia, Universidade Técnica de Lisboa, Lisbon, Portugal

Abstract

The oxygen stable isotope composition ($\delta^{18}O$) of CO_2 is a valuable tool for studying the gas exchange between terrestrial ecosystems and the atmosphere. In the soil, it records the isotopic signal of water pools subjected to precipitation and evaporation events. The $\delta^{18}O$ of the surface soil net CO_2 flux is dominated by the physical processes of diffusion of CO_2 into and out of the soil and the chemical reactions during CO_2–H_2O equilibration. Catalytic reactions by the enzyme carbonic anhydrase, reducing CO_2 hydration times, have been proposed recently to explain field observations of the $\delta^{18}O$ signatures of net soil CO_2 fluxes. How important these catalytic reactions are for accurately predicting large-scale biosphere fluxes and partitioning net ecosystem fluxes is currently uncertain because of the lack of field data. In this study, we determined the $\delta^{18}O$ signatures of net soil CO_2 fluxes from soil chamber measurements in a Mediterranean forest. Over the 3 days of measurements, the observed $\delta^{18}O$ signatures of net soil CO_2 fluxes became progressively enriched with a well-characterized diurnal cycle. Model simulations indicated that the $\delta^{18}O$ signatures recorded the interplay of two effects: (1) progressive enrichment of water in the upper soil by evaporation, and (2) catalytic acceleration of the isotopic exchange between CO_2 and soil water, amplifying the contributions of 'atmospheric invasion' to net signatures. We conclude that there is a need for better understanding of the role of enzymatic reactions, and hence soil biology, in determining the contributions of soil fluxes to oxygen isotope signals in atmospheric CO_2.

Keywords: atmospheric invasion, carbonic anhydrase, drought, Mediterranean forests, oxygen isotopes, *Quercus suber*, soil CO_2 efflux, soil evaporation, soil water $\delta^{18}O$ composition

Received 14 November 2007 and accepted 14 February 2008

Introduction

The $^{18}O/^{16}O$ ratio of CO_2 has gained attention as a tracer for CO_2 fluxes at the ecosystem (Yakir & Wang, 1996; Riley *et al*., 2002, 2003; Bowling *et al*., 2003; Ogée *et al*., 2004) and global scales (Farquhar *et al*., 1993; Peylin *et al*., 1999; Cuntz *et al*., 2003a, b). It might also provide a constraint on the role evapotranspiration plays in the atmospheric energy balance, especially at the continental scale (Tans, 1998). This is because large differences in the oxygen isotope signatures of leaf and soil gas exchange exist, thereby lending itself as an independent tool to assess the contribution of photosynthetic and respiratory fluxes to the net ecosystem exchange during the day and the respiratory contribution of foliage, stem and soil components to the nocturnal net ecosystem exchange. The oxygen isotope composition of CO_2 released from soils is determined by the interplay between diffusion of CO_2 into and out of the soil and isotopic equilibration of the CO_2 with soil water (Hesterberg & Siegenthaler, 1991). As soil water is continuously subjected to precipitation, evaporation and condensation, isotopic signals from such processes should be transferred to the oxygen isotope composition of CO_2 leaving soils. Acceleration of the CO_2–water equilibration catalyzed by carbonic anhydrase (CA; also noted EC 4.2.1.1) in the soil has been suggested to explain field observations (Seibt *et al*., 2006). The

Correspondence: Lisa Wingate, e-mail: l.wingate@ed.ac.uk

enzyme reaction enhances the equilibration of CO_2 that diffuses into and out of the soil ('atmospheric invasion') without affecting net soil CO_2 fluxes. Model simulations indicate that this could have large effects on CO_2 isotopic signals from the soil (Riley *et al*., 2002; Seibt *et al*., 2006). Such variations could contribute to a dynamic pattern in the $\delta^{18}O$ signal of the net soil CO_2 flux on timescales of hours to season. However, implications for accurately predicting larger scale biosphere fluxes and partitioning net fluxes are uncertain because of a lack in field data.

Mediterranean soils experience extremes of water content at the soil surface over particularly short time periods (days) (Jarvis *et al*., 2007). This makes them ideal systems to study the signals water cycling imparts on the oxygen isotope composition of atmosphere–biosphere CO_2 exchange. More generally, Mediterranean ecosystems are characterized by the occurrence of various stresses, particularly drought and high temperature. Significant climatic shifts are expected for Mediterranean areas, particularly changes in the distribution of rainfall and increases in the evaporative demand by the atmosphere (Miranda *et al*., 2002; Pereira *et al*., 2007). While predictions for average annual temperature change in the Mediterranean Basin agree on a 2–3 °C increase by 2050 (Cubash *et al*., 1996), the direction and magnitude of precipitation change remain more uncertain. However, in the Iberian Peninsula, the most likely future scenarios include longer dry seasons (Miranda *et al*., 2002). A thorough understanding of the impacts of such changes on Mediterranean ecosystems will be crucial for their future management (Lavorel *et al*., 1998).

In this study, we examined the diurnal variations in the $\delta^{18}O$ signatures of the net soil CO_2 fluxes from a Mediterranean forest soil during a 3-day study in April 2005. We collected air samples from automated open soil chambers and analysed them with respect to the mole fraction and the oxygen isotope composition of CO_2. From these data, we calculated the net soil CO_2 fluxes and their isotopic signatures. We also measured soil properties and collected soil samples to determine the isotope composition of the water pools that were likely to affect the isotope composition of CO_2 fluxes. We then used a model of soil gas exchange to assess the effects of evaporation, diffusion and biological controls on oxygen isotope signals transferred from droughted soils to the atmosphere.

Materials and methods

Site description

The study took place in Herdade da Mitra (38°32′N, 8°01′W, 221 m a.s.l.), 12 km southwest of Évora in southern Portugal. The climate is typically Mediterranean, with a hot and dry summer. Most precipitation occurs between October and April. The experimental plot was an acid litholic nonhumic soil derived from Gneiss with a pH of 4–6 (David, 2000), on a 5° slope. A 25-m-deep borehole was drilled 500 m away from the experimental area, from which soil and geological profiles were characterized (David, 2000). From the surface to 1 m depth, the soil consisted of 89% sand, 5% silt and 6% clay, with a water retention capacity of 5% ($pF_{2.5} = 8$ and $pF_{4.2} = 3$). The experimental plot encompassed an area of 0.264 ha (46 m × 60 m) exclusively covered with *Quercus suber* L. trees planted in 1988, with an understorey composed of *Cistus salvifolius* L. and *Cistus crispus* L. and herbaceous plants (mostly winter–spring C3 annuals).

At the end of the field campaign, a pit transect (3.6 m × 1.4 m × 1.5 m) was dug nearby the experimental plot to characterize and quantify root biomass from the different vegetation types (grass, shrubs and trees). From this transect, three soil profiles were collected vertically with samples every 0.1 m down to 1 m depth. The majority of root biomass was observed at 0.2, 0.4 and 0.9 m depth, with 19%, 13% and 17%, respectively, of the total root biomass measured at these depths (Kurz-Besson *et al*., 2006).

Meteorological and flux measurements

Weather conditions were continuously recorded at a meteorological station set up at the field site. Precipitation, air humidity and temperature above the canopy were measured every 5 min, averaged and logged every 30 min to a data logger. Soil water status beneath each soil chamber was monitored daily throughout the field campaign at depths of 10, 20, 30, 40, 60 and 100 cm using a PR2 Profile Probe attached to a HH2 moisture meter (Delta-T Devices Ltd, Cambridge, UK). Soil temperature was recorded beneath soil chamber 1 at a depth of 0, 2.5, 5, 10, 20 and 30 cm, while the soil temperature beneath soil chamber 3 was only measured at 5 and 20 cm depth. The average and SD of measured temperature were stored every 15 min.

Soil surface CO_2 efflux

An automatic open-chamber soil respiration system was deployed in the experimental plot. The soil chambers operated as an open gas exchange system, i.e. the net CO_2 flux was calculated from the difference in the CO_2 concentration between the air flowing into and out from the chamber, and the flow rate (Rayment & Jarvis, 1997).

In brief, the soil chambers consisted of a closed cylindrical chamber (diameter 0.28 m) attached to a round collar constructed from aluminium sheet (Fig. 1). Air was pumped at a flow rate of 1 $dm^3 min^{-1}$ from the chamber

through a peripherally mounted perforated tube followed by: an in-line dessicator; an eight-way solenoid; a 25-mm PTFE membrane of 1 μm pore size housed within a 25 mm in-line filter holder [Delrin®, Du Pont (UK) Ltd, Herts, UK]; a mass flow meter (FM360 4S, Viton Range, 2.5 s.l.p.m. for Air, Millipore Ltd, Watford, UK) and a polycarbonate flow meter before reaching the infra-red gas analyser (CIRAS-DC, PP Systems, Hitchin, UK).

Between measurements, the pneumatically actuated chambers were raised above the soil surface to minimize disturbances in the water and energy balance of the soil inside the chamber. The seal between the chamber and collar was maintained with a PVC/sponge rubber sealing strip around the collar. Each chamber was sampled for 15 min. Both the reference and sample air streams were passed through drying columns containing magnesium perchlorate within 1 m of the chamber to prevent condensation of water vapour in the lines. The flow rates of the two air streams were also output to the data logger for flux calculation.

$\delta^{18}O$ of net soil CO_2 flux

Reference and sample air was collected every 2 h for about 72 h on two soil chambers. A glass flask of 0.2 dm^3 was placed in-line on each air stream immediately after the soil chamber ($\leq$1 m) and drying column containing $Mg(ClO_4)$. Tubing was inserted inside a glass side arm and secured to Cajon fittings that allowed complete flushing of the flasks (Fig. 1). For a full description of the flasks and tubing set-up, refer to Hemming *et al*. (2005). Flasks were placed in-line before the soil chamber lid closed and flushed with the air stream until about 20 s before the chamber opened again at which point the inner tubes were retracted from the flasks and the vacuum stopcocks closed. The $\delta^{18}O$ of CO_2 in air was then analysed at the Weizmann Institute for Science using the continuous flow mass spectrometer configuration described in Kapiluto *et al*. (2007).

Calculations of $\delta^{18}O$ signatures of soil CO_2 exchange

During the 15-min chamber closure period, steady-state gas exchange was verified visually in the field using a laptop connected to a datalogger before the glass flasks were taken and the chambers re-opened. The oxygen isotope signal of the net CO_2 fluxes during chamber closure ($\delta^{18}O_{ch}$) was calculated using a simple isotopic mass balance:

$$\delta^{18}O_{ch} = \frac{\delta^{18}O_o C_o - \delta^{18}O_i C_i}{C_o - C_i}, \qquad (1)$$

where C_o, C_i and $\delta^{18}O_o$, $\delta^{18}O_i$ are the mole fractions and isotopic compositions of CO_2 in the air leaving and entering the chamber, respectively.

Soil and ground water $\delta^{18}O$ composition

Soil samples were collected at the same time of day (around 14:00 UT) for 3 days at four depths (0–5, 5–10, 10–15 and 15–20 cm depth) in the vicinity (within 30 cm) of the soil chambers. The $\delta^{18}O$ analysis of extracted soil water was completed at the Weizmann Institute of Science as described in Kapiluto *et al*. (2007).

Model description

We used a one-dimensional numerical model that simulates the production, diffusion and equilibration of CO_2 in the soil and the resulting depth profiles of soil CO_2 and $C^{18}O^{16}O$. All symbols and units used are presented in Table 1. The transient depth-dependent concentration of soil CO_2, C_s [μmol(CO_2) m^{-3}], was calculated as follows:

$$\frac{\partial((\theta_a + B\theta_w)C_s)}{\partial t} = \frac{\partial}{\partial z}\left(D_s \frac{\partial C_s}{\partial z}\right) + S_c, \qquad (2)$$

where θ_a and θ_w ($m^3\,m^{-3}$ soil) are the volumetric soil air and moisture content, B (m^3 air m^{-3} water) is the temperature-dependent Bunsen solubility coefficient, S_c [μmol(CO_2) $m^{-3}\,s^{-1}$] is the depth-dependent CO_2

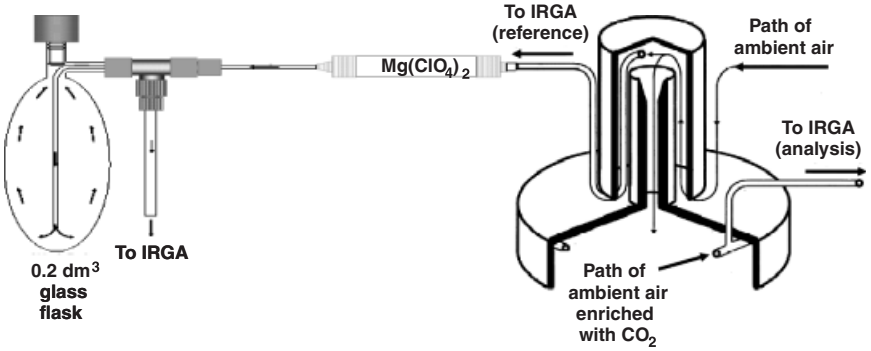

Fig. 1 Schematic of soil chamber and flow of air through the chamber, drying column and glass flask. N.B. glass flask only shown for reference line but also present on the analysis line. Soil chamber picture courtesy of M. B. Rayment.

Table 1 Symbols used in the text

Symbols used in the text		
α_d	Kinetic fractionation factor ($= 1 + \varepsilon_d$)	‰
α_{eq}	Equilibrium fractionation factor ($= 1 + \varepsilon_{eq}$)	‰
B	Bunsen solubility coefficient	m^3 air m^{-3} water
b	Slope of the water retention function	4.9
C_a	CO_2 mole fraction in ambient air	$\mu mol\,mol^{-1}$
C_i	CO_2 mole fraction of air entering the chamber	$\mu mol\,mol^{-1}$
C_o	CO_2 mole fraction of air leaving the chamber	$\mu mol\,mol^{-1}$
C_s	CO_2 mole fraction in the soil reservoir	$\mu mol\,m^{-3}$
$\delta^{18}O$	Oxygen isotope composition $(\Re_{sample}/\Re_{standard} - 1) \times 1000$	‰
$\delta^{18}O_a$	Oxygen isotope composition of ambient air (chamber reference airstream)	‰
$\delta^{18}O_{ch}$	Observed or modelled oxygen isotope composition of the net soil CO_2 flux in chambers [Eqn (1)]	‰
$\delta^{18}O_{eq}$	Oxygen isotope composition of CO_2 in full equilibration with soil water	‰
$\delta^{18}O_{flux}$	Modelled oxygen isotope composition of the net soil CO_2 flux [Eqn (5)]	
$\delta^{18}O_{gw}$	Oxygen isotope composition of groundwater	‰
$\delta^{18}O_i$	Oxygen isotope composition of CO_2 entering the chamber	‰
$\delta^{18}O_s$	Oxygen isotope composition of CO_2 in soil air	‰
$\delta^{18}O_{sw}$	Oxygen isotope composition of soil water	‰
$\delta^{18}O_o$	Oxygen isotope composition of CO_2 leaving the chamber	‰
D_s	Effective diffusivity of CO_2 in soil air	$m^2\,s^{-1}$
D_s^{18}	Diffusivity of $C^{18}O^{16}O$ in soil air	$m^2\,s^{-1}$
D_{25}	Molecular diffusivity of CO_2 at 25 °C	$1.410^{-5}\,m^2\,s^{-1}$
ε_d	Full diffusive fractionation	−8.7‰
ε_{eq}	Equilibrium fractionation at the local soil temperature	‰
f_{CA}	Factor modifying the hydration rate	
H	Relative humidity	%
k_h	Hydration rate	s^{-1}
k_s	Effective hydration rate	s^{-1}
n	Exponent in diffusivity expression	1.5
pF_x	Logarithm of the free energy difference	cm
R_s	Measured net soil CO_2 flux	$\mu mol\,m^{-2}\,s^{-1}$
$\Re_c$	Oxygen isotope ratio of the respired CO_2	
$\Re_{eq}$	Oxygen isotope ratio of CO_2 in isotopic equilibrium with the surrounding soil water	
$\Re_s$	Oxygen isotope ratio of the CO_2 in soil air	
$\Re_{sw}$	Oxygen isotope ratio of soil water	
$\Re_{VPDB\text{-}CO_2}$	Oxygen isotope ratio of the standard VPDB-CO_2	
S_c	Depth-dependent CO_2 production rate	$\mu mol\,m^{-3}\,s^{-1}$
T_a	Air temperature	°C
T_s	Soil temperature	K
T_5	Soil temperature at 5 cm soil depth	°C
T_{25}	Temperature 25 °C expressed in Kelvin	K
θ_a	Soil air content	$m^3\,m^{-3}$ soil
θ_{sat}	Saturated water content	$m^3\,m^{-3}$ soil
θ_w	Soil moisture content	$m^3\,m^{-3}$ soil
z	Depth	m

production rate and t and z are time and depth, respectively. The effective diffusivity of CO_2 in soil air, D_s ($m^2\,s^{-1}$), was calculated following Moldrup *et al.* (2003) as follows:

$$D_s = D_{25}\theta_a^2\left(\frac{\theta_a}{\theta_{sat}}\right)^{3/b}\left(\frac{T_s}{T_{25}}\right)^n, \qquad (3)$$

where D_{25} is the molecular diffusivity of CO_2 at 25 °C ($1.410^{-5}\,m^2\,s^{-1}$), T_s (K) is the soil temperature, θ_{sat} ($0.3\,m^3\,m^{-3}$ soil) is the saturated water content, n is 1.5 (Bird *et al.*, 2002) and b is the slope of the water retention function, estimated here as 4.9 (Kurz-Besson *et al.*, 2006).

We calculated the transient depth-dependent concentration of $C^{18}O^{16}O$ in the soil as follows:

$$\frac{\partial((\theta_a + B\theta_w)\Re_s C_s)}{\partial t} = \frac{\partial}{\partial z}\left[D_s^{18}\frac{\partial(\Re_s C_s)}{\partial z}\right] + \Re_c S_c + k_s B\theta_w C_s(\Re_{eq} - \Re_s), \quad (4)$$

where $\Re_s$, $\Re_c$ and $\Re_{eq}$ are the $^{18}O/^{16}O$ ratios of the CO_2 in soil air, respired CO_2, and CO_2 in isotopic equilibrium with the surrounding soil water: $\Re_{eq} = \alpha_{eq}\Re_{sw}$. $\alpha_{eq} = 1 + \varepsilon_{eq}$ is the equilibrium fractionation and depends on soil temperature: $\varepsilon_{eq} = (17\,604/T_s - 17.93)/1000$ (Brenninkmeijer *et al.*, 1983). The effective diffusivity of $C^{18}O^{16}O$ in soil air was calculated as $D_s^{18} = D_s\,\alpha_d$, where $\alpha_d = 1 + \varepsilon_d$, using the kinetic fractionation ε_d of −8.7‰ (Tans, 1998). The temperature-dependent hydration rate k_h (s^{-1}) was equal to one-third the hydration rate because there are three oxygen atoms present in the bicarbonate intermediate: $k_h = 1/3 \times 0.037 \times \exp[0.118(T_s - T_{25})]$. This rate was modified to account for the potential acceleration of CO_2 hydration rates due to the activity of the enzyme carbonic anhydrase (CA) in the soil (Riley *et al.*, 2003). The effective rate of isotopic exchange was then calculated as $k_s = f_{CA}k_h$, where f_{CA} expresses the relative increase in hydration rate due to CA activity. The three terms in Eqn (4) describe the diffusion, production and equilibration of $C^{18}O^{16}O$ in the soil.

The influence of the soil chamber on soil profiles was accounted for by using a finite air volume (virtual chamber) as the boundary condition at the soil surface (Seibt *et al.*, 2006). This is necessary to correctly interpret chamber measurements. Thus, a distinction is made between the oxygen isotope composition of the net soil CO_2 flux without a chamber (denoted $\delta^{18}O_{flux}$ hereafter) and that with a chamber (denoted $\delta^{18}O_{ch}$). Using this boundary condition at the soil surface, and initial conditions inside the chamber $C = C_i$ and $\delta = \delta_i$, Eqns (3) and (4) are then solved numerically as described in Appendix A, and the net CO_2 and $C^{18}OO$ fluxes are computed from gradients at the soil surface multiplied by their respective effective diffusivities. The predicted oxygen isotope composition of the net soil CO_2 flux before chamber closure is then computed as follows:

$$\delta^{18}O_{flux} = \frac{\left.\frac{\partial C_s\delta^{18}O_s}{\partial z}\right|_{z=0,\,t=t_0}}{\left.\frac{\partial C_s}{\partial z}\right|_{z=0,\,t=t_0}} + \varepsilon_d, \quad (5)$$

where $\delta^{18}O_s = \Re_s/\Re_{VPDB\text{-}CO_2} - 1$, $\varepsilon_d = D_s^{18}/D_s - 1$ and t_0 is the time before chamber closure (Figs 2 and 3). The same equation, but taken at $t > t_0$ is also used to compute the transient isotopic signature of the soil CO_2 flux inside the chamber (noted $\delta^{18}O_{ch}$ in Fig. 3). However, because the model predicts the transient time course of C and δ inside the chamber (Fig. 3), Eqn (1) can also be used, with predicted values of C_o and δ_o, and thereby observations and modelled $\delta^{18}O_{ch}$ are directly comparable.

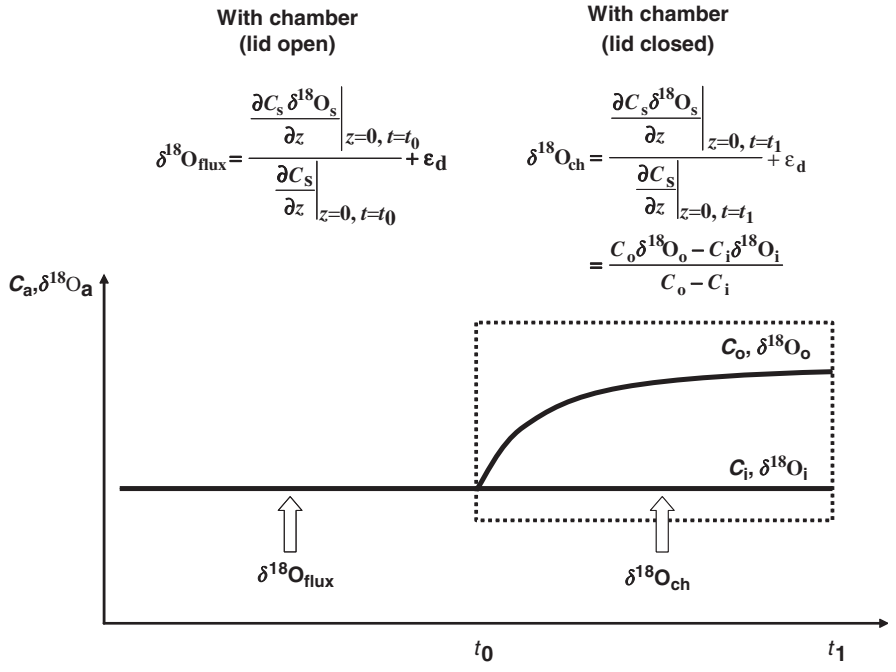

Fig. 2 Differences between the oxygen isotopic composition of the net soil CO_2 flux with and without chambers.

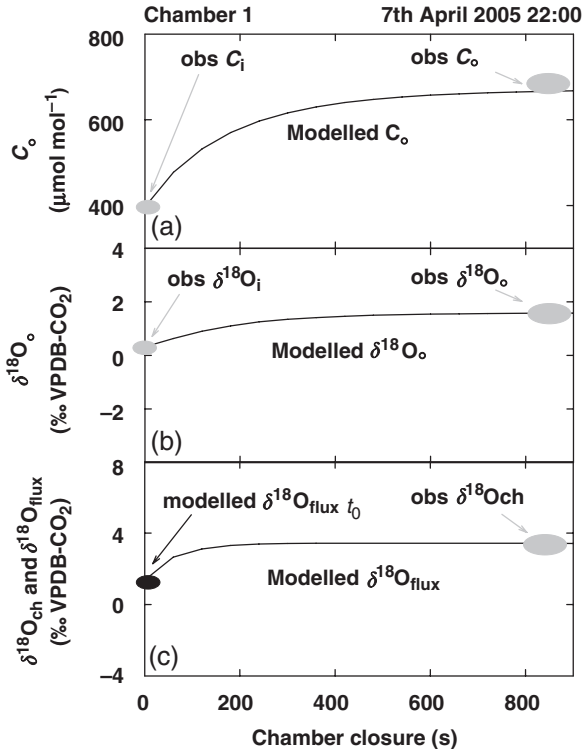

Fig. 3 Example of chamber flask measurements (solid grey ellipses) plotted against (a) the transient buildup of modelled CO_2 mole fraction (C_o, solid line); (b) the oxygen isotope composition of air in the chamber ($\delta^{18}O_o$, solid line); and (c) the transient oxygen isotope composition of the net CO_2 flux modelled inside the chamber ($\delta^{18}O_{ch}$, solid line) alongside the flask observed $\delta^{18}O_{ch}$ and the modelled oxygen isotope composition of the soil net CO_2 flux in the absence of chambers ($\delta^{18}O_{flux}$, black ellipse) for the closure period 7 April 2005, 22:00 hours, in Chamber 1.

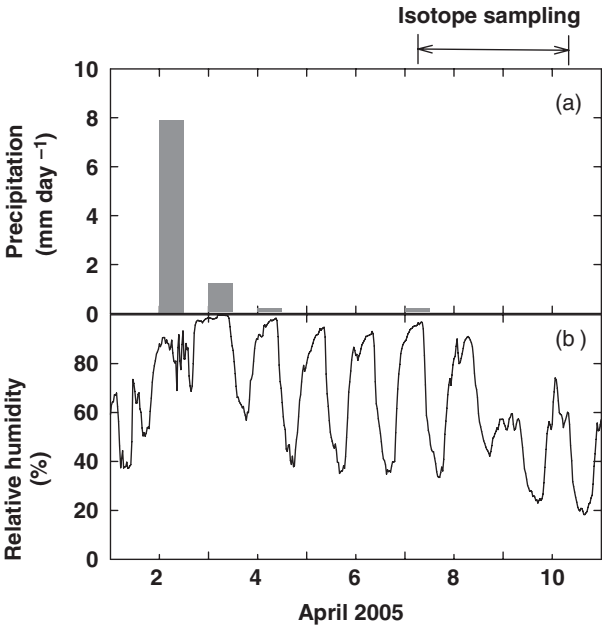

Fig. 4 Time series of measured (a) precipitation and (b) relative humidity measured before and during the isotope field campaign.

Results

Field data

Before our isotope sampling campaign, a 9-mm rain event occurred over the 2 and 3 April 2005 (Fig. 4a). This rain pulse was typical for the region and was followed by dry, warm, sunny conditions during the day for the duration of the field campaign. Over the 3-day isotope sampling campaign, nocturnal relative humidity varied by about 40% with humid conditions dominating on the first night of the campaign, followed by less humid conditions on the last two nights (Fig. 4b). This was accompanied by peak daytime humidity ranging from about 45% on the first day to about 20% by the last.

Profiles of soil volumetric water content measured beside the two soil chambers were quite different, with chamber 1 exhibiting a much drier profile in the upper 40 cm of about 4–6% (Fig. 5). In contrast, chamber 2 had a dry layer in the top 10 cm of about 7–8%, then increasing in moisture content to 12–18% between 20 and 40 cm. Over the 3-day campaign, there were small decreases in the moisture content in the top 40 cm of the profile.

During the sampling period, a strong diurnal pattern in the measured net CO_2 flux (R_s) was observed (Fig. 6). This pattern in R_s consistently tracked the diurnal swings in temperature measured 5 cm beneath the soil chambers, with a nearly 8 °C peak-to-peak difference between the morning and early evening period. Values of R_s correspondingly varied between 2.5 and 4.5 μmol m^{-2} s^{-1} over the field campaign and were similar for both soil chambers.

The CO_2 mole fraction (C_i) and $\delta^{18}O$ values of atmospheric CO_2 ($\delta^{18}O_i$) surrounding the soil chambers were determined from flask samples collected from the air stream entering the soil chamber (Figs 1 and 7). A diurnal pattern was apparent for C_i, reflecting the nocturnal buildup of CO_2 beneath the canopy during calm periods, especially around the periods of midnight on the 7 and 9 of April (Fig. 7a). However, windy conditions during the early mornings of the 8 and 9 April minimized CO_2 buildup beneath the canopy. Values of $\delta^{18}O_i$ showed no obvious diurnal cycle during the field campaign (Fig. 7b). The observed oxygen isotope signatures of net soil CO_2 fluxes in chambers ($\delta^{18}O_{ch}$) varied displaying a gentle diurnal cycle

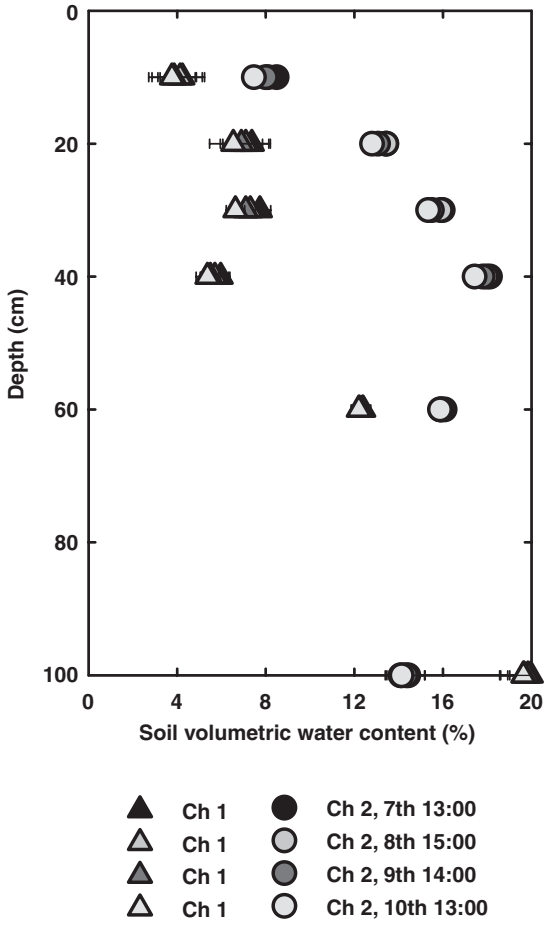

Fig. 5 Observed variations in soil volumetric water content (expressed as a %) with depth (cm) adjacent to chambers 1 (triangles) and 2 (circles) over the field campaign.

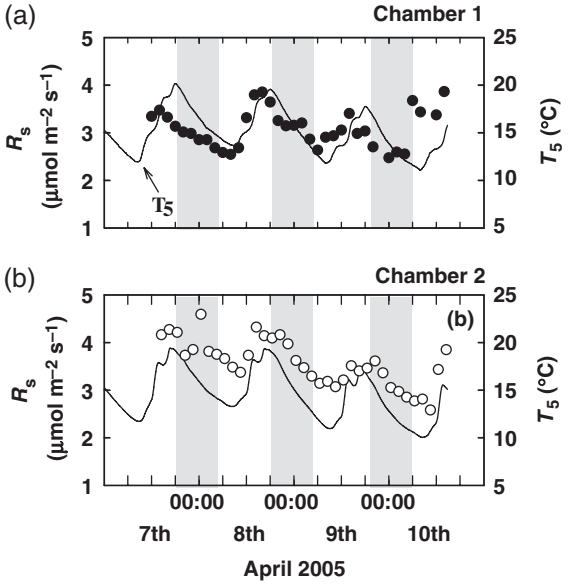

Fig. 6 Time-series observations from chambers 1 and 2 (a and b, respectively) for soil temperature at 5 cm (solid line) soil depth alongside the observed net soil CO_2 flux (circles).

(Fig. 7c). Furthermore, over the 3-day study, an enrichment of about 12‰ was observed in $\delta^{18}O_{ch}$ for both chambers.

Numerical modelling

As the oxygen isotope composition of the net soil CO_2 flux is affected by a number of interacting processes, we used the numerical model described earlier to investigate the response of the observed system to changes in the prevailing environmental conditions. The model was also employed to perform sensitivity analysis on different parameters.

The $\delta^{18}O_{sw}$ profile was defined by fitting exponential functions with e-folding depths of 6 and 8 cm to the data (Fig. 8 and Table 2). For the model boundary at 1 m depth, we used the isotopic composition of groundwater (−5.4‰ VSMOW) measured at the site during the sampling campaign.

We performed a series of model simulations combining constant or increasing $\delta^{18}O_{sw}$ conditions at the soil surface accompanied with and without an enhanced rate of CO_2 hydration (f_{CA}) in the soil (Table 2). Main results from our simulations are presented in Fig. 9, including

- *Scenario 1*: a constant $\delta^{18}O_{sw}$ over time ($\delta^{18}O_{sw}$: 3‰ or 6‰ VSMOW) and no enhanced hydration rate ($f_{CA} = 1$);
- *Scenario 2*: a linear increase in $\delta^{18}O_{sw}$ of 3‰ at the surface over the study period and no enhanced hydration rate ($f_{CA} = 1$);
- *Scenario 3*: a constant $\delta^{18}O_{sw}$ over time ($\delta^{18}O_{sw}$: 3‰ or 6‰ VSMOW) and an enhanced hydration rate ($f_{CA} = 300$) and finally
- *Scenario 4*: a linear increase in $\delta^{18}O_{sw}$ of 3‰ at the surface over the study period and different rates of enhanced hydration ($f_{CA} = 50$, 100 or 300).

For scenarios 3 and 4, the enhanced hydration rate ($f_{CA} > 1$) was applied in the surface soil layers. For the sake of clarity, we only plot the data and simulations for chamber 2 in the different panels of Fig. 9.

It was obvious from the results of Scenario 1 that the predicted oxygen isotope composition of the net soil CO_2 flux in chambers ($\delta^{18}O_{ch}$) could not capture the field observations at all (Fig. 9). The most striking result from this simulation was that the model output was offset from the field data by about 10‰ at the start of the

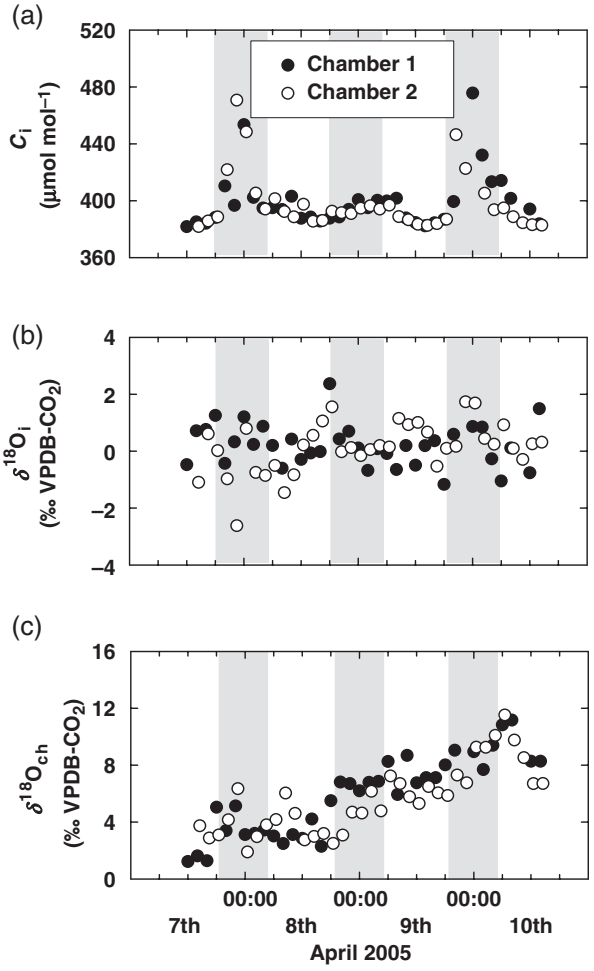

Fig. 7 Time-series observations from chambers 1 (filled circles) and 2 (open circles) of (a) flask CO_2 mole fraction (C_i), (b) the oxygen isotope composition of flask CO_2 collected in the soil chamber reference airstream ($\delta^{18}O_i$) and the observed oxygen isotope signatures of the net soil CO_2 flux ($\delta^{18}O_{Ch}$) over the field campaign.

field campaign. This offset gradually increased to nearly 17‰ by the end. Moreover, these predicted values were opposite in sign to the observations. Scenario 1 also failed to replicate the increasing trend in $\delta^{18}O_{ch}$ observed for both chambers over the study period.

Incorporating the evaporative enrichment prescribed in Scenario 2 made little impact on the offset between observations and predictions (Fig. 9). This simulation resulted in an overall enrichment of less than 5‰ in modelled $\delta^{18}O_{ch}$ over the 3 days (i.e. much smaller than the observed trend of about 12‰). Using the model and assuming no enhanced hydration rate of CO_2, we sought the composition of soil water required to explain our observations. We found that values for $\delta^{18}O_{sw}$ between the range of 30‰ and 50‰ would be necessary to explain our field observations. This level of enrichment in $\delta^{18}O_{sw}$ in natural systems is unrealistic. From Scenarios 1 and 2, we conclude that the processes of diffusion, production, chemical equilibration and evaporation alone cannot account for the observed values of $\delta^{18}O_{ch}$.

In Scenario 3, we increased the hydration rate of soil CO_2 (f_{CA}). Good agreement between model and observations is achieved with an f_{CA} of about 300. The scenario captured the observed values and sign (Fig. 9). If only f_{CA} is included, but $\delta^{18}O_{sw}$ held constant at 3‰, it is possible to achieve agreement with the data for the first day. However, during the second and third day, predictions and observations began to diverge by up to 5‰ and 8‰, respectively (Fig. 9). In other words, with constant $\delta^{18}O_{sw}$ and enhanced f_{CA}, it is not possible to match the observed strong temporal trend in the field observations at the same time. Lastly, in Scenario 4, both an accelerated rate of CO_2 hydration and an evaporative enrichment of $\delta^{18}O_{sw}$ at the soil surface achieved a good fit between modelled and observed $\delta^{18}O_{ch}$ (Fig. 9). This model scenario also captured well some of the finer structure in the temporal dynamics of the observed signal. Therefore, we clearly require an enhanced rate of hydration and a modest evaporative enrichment in $\delta^{18}O_{sw}$ to explain our field results.

A summary of the above results for both chambers is provided in Fig. 10, which compares observed and predicted oxygen isotope signatures of the net CO_2 flux. If we assume a similar top soil surface water enrichment for both chambers (from 1.4‰ to 5.7‰ VSMOW), an f_{CA} of 400 for chamber 1 and about 300 for chamber 2 is needed to explain our data. However, chamber 1 was situated in a drier plot than chamber 2 (Fig. 5), and therefore, it is likely that the top soil surface $\delta^{18}O_{sw}$ of chamber 1 was more enriched compared with that of chamber 2. Using values of 2.7–6.9‰ VSMOW (instead of 1.4–5.7‰) for chamber 2 and an identical f_{CA} of 450 would also provide a very good fit to both sets of observations ($r^2 = 0.76$, $P < 0.001$), as shown in Fig. 10.

Discussion

Physiologically essential need for an increased rate of CO_2 hydration in soil dwelling organisms

Our study indicates an accelerated isotopic equilibration of CO_2 with soil water, beyond that predicted by a purely abiotic description of soil gas exchange processes. We hypothesize that our results are explained by the catalytic action of carbonic anhydrase on the hydration rate of CO_2. This has also been proposed for a peaty gley soil in a temperate spruce forest (Seibt *et al.*,

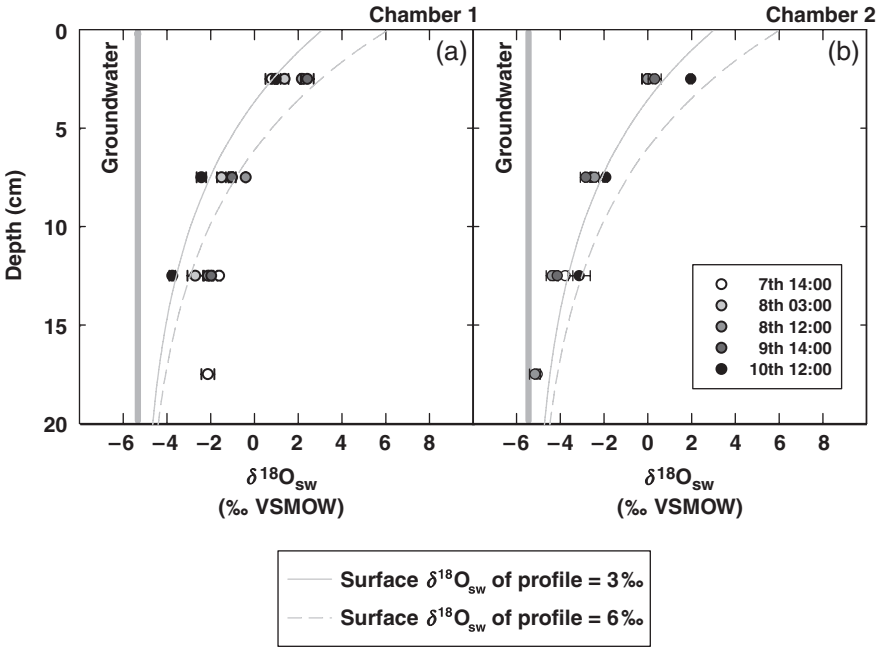

Fig. 8 Measured groundwater ($\delta^{18}O_{gw}$) and soil water ($\delta^{18}O_{sw}$) oxygen isotope composition ±1 SD at four depths over 5 consecutive days for each chamber. Alongside, the predicted profiles are plotted for two scenarios of $\delta^{18}O_{sw}$ at the surface of the soil. $\delta^{18}O$ values are relative to the VSMOW standard. Each value represents the mean of two replicates.

Table 2 Parameter values used in the model sensitivity analysis illustrated in Fig. 9

Chamber no.	Soil surface $\delta^{18}O$ (‰ VSMOW)	f_{CA}
Scenario 1 – Constant $\delta^{18}O_{sw}$		
Chamber 1	3 and 6	1
Chamber 2	3 and 6	1
Scenario 2 – Variable $\delta^{18}O_{sw}$		
Chamber 1	t_0–t_{72} = 3–6; 30–50	1
Chamber 2	t_0–t_{72} = 3–6; 30–50	1
Scenario 3 – Constant $\delta^{18}O_{sw}$ + f_{CA}		
Chamber 1	3 and 6	300
Chamber 2	3 and 6	300
Scenario 4 – Variable $\delta^{18}O_{sw}$ + constant f_{CA}		
Chamber 1	t_0–t_{72} = 3–6	50 100 300
Chamber 2	t_0–t_{72} = 3–6	50 100 300

2006). In the following, we detail biochemical pathways requiring CA which are necessary for soil microbes to (1) fulfil their growth requirements when limited resources become temporarily available and (2) function effectively in response to environmental stresses such as drought. These pathways are illustrated using examples from Mediterranean soil ecology. However, they are by no means unique to this particular ecosystem and are likely to play a role in the soil environment of many other biomes.

Bicarbonate that forms the substrate for a number of carboxylation reactions (Raven & Newman, 1994) cannot easily diffuse across most cell membranes (Gutknecht *et al.*, 1977). In contrast, CO_2 is highly soluble in both aqueous solutions and lipids and can diffuse more easily through biological membranes. Once CO_2 has diffused through the membrane, it is then hydrated to bicarbonate. This hydration is a slow process though, with a half time of about 14 s. In plants, bacteria and fungi, many of their carboxylating pathways require the presence of CA to ensure that the hydration to HCO_3^- is sufficiently faster than the rate at which CO_2 diffuses out of the cell. These pathways are summarized in Table 3. Although sufficient CO_2 is produced during catabolism, deprivation of atmospheric CO_2 leads to growth inhibition and death of heterotrophs (Brown & Howitt, 1969; Dehority, 1971). Carbonic anhydrase is expressed in abundance by many soil dwelling organisms such as bacteria (Kozliak *et al.*, 2000; Kusian *et al.*, 2002; Mitsuhashi *et al.*, 2004) and fungi (Aguilera *et al.*, 2005; Amoroso *et al.*, 2005; Klengel *et al.*, 2005; Mogensen *et al.*, 2006). The wide occurrence of CA in bacteria and fungi indicate a fundamental physiological significance of these enzymes in dissolved inorganic carbon (DIC) metabolism in cells. Carbonic anhydrase is also found in most compartments of plant cells, including nonphotosynthetic organs and tissues (Raven & Newman, 1994). For instance, it has been found in the roots of plants (Viktor

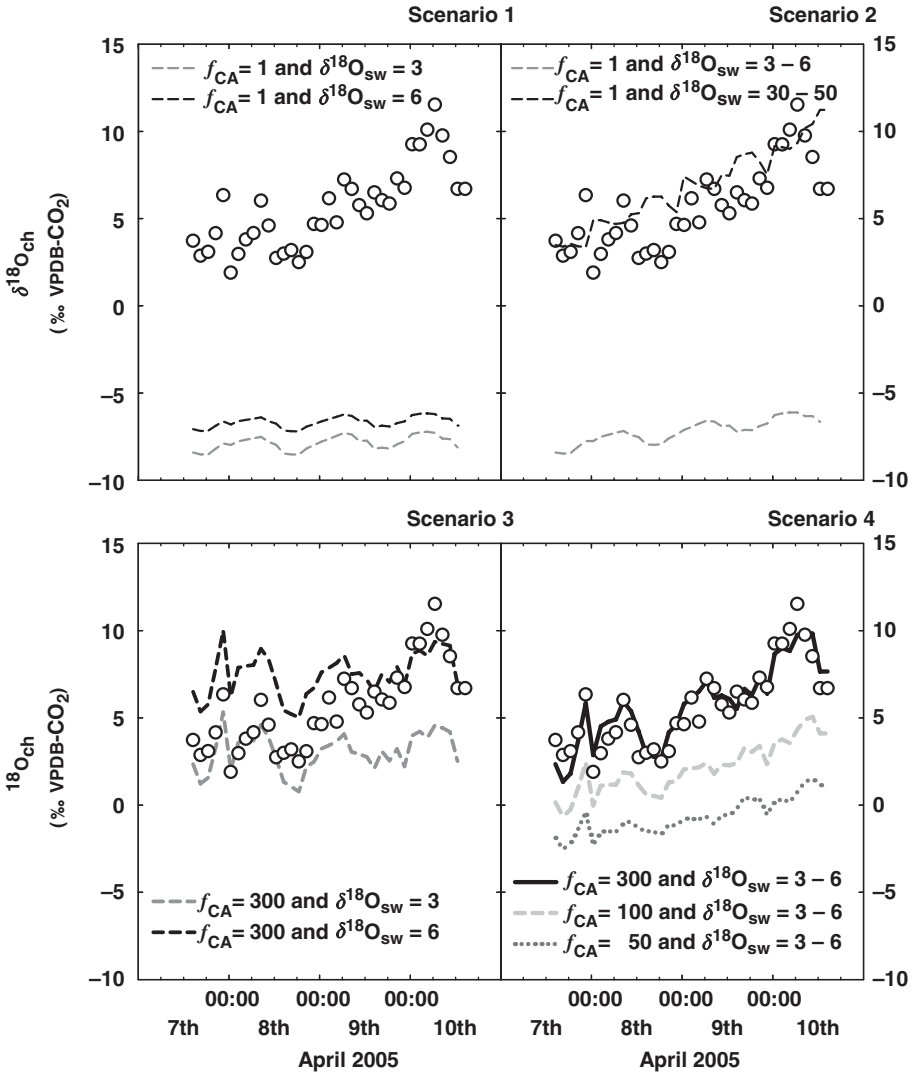

Fig. 9 Sensitivity analysis for the predicted oxygen isotope signatures of the net soil CO_2 flux ($\delta^{18}O_{pred}$) exploring the effect of constant or variable $\delta^{18}O_{sw}$ at the surface with $f_{CA} > 1$ and without an enhanced rate of CO_2 hydration, i.e. $f_{CA} = 1$, as described in Table 2. Model time series (lines) are plotted alongside the observed oxygen isotope signatures of the net soil CO_2 flux ($\delta^{18}O_{Ch}$) for chamber 2 only (open circles), collected during April 2005.

& Cramer, 2005) and extremely high activities (200 times in excess of 'apparent' metabolic demands for DIC) were observed in growing root tips of *Zea mays* L. (Chang & Roberts, 1992). Further indirect evidence for the presence of CA in soils comes from observations of carbonyl sulphide (COS) uptake by litter (Kesselmeier & Hubert, 2002) and soils in a number of biomes (Conrad, 1996; Kesselmeier *et al*., 1999; Simmons *et al*., 1999; Steinbacher *et al*., 2004; Van Diest & Kesselmeier, 2007), including Mediterranean oak woodlands (Kuhn *et al*., 1999). COS uptake is an indicator of CA activity because carbonyl sulphide also reacts with CA as a structural analogue of CO_2 catalyzing the hydrolysis of COS to CO_2 and H_2S. On the basis of the above evidence, we suggest that CA is present and functional in numerous organisms inhabiting the soil.

Direct evidence for the presence of CA in soils is sparse, with only a few studies attempting to quantify its presence and activity. Studies so far have been confined to karst ecosystems, where the presence of CA (both intra- and extracellular) in soil bacteria and leachates from soil columns has been implicated in the enhanced dissolution of limestone (Li *et al*., 2004, 2005). Li *et al*. (2005) found that CA activity in leachates correlated with an increase in Ca^{2+} concentrations, thus also releasing a potential source of bicarbonate to the microbes. Assessing CA activity using methods similar to the studies above was unfortunately beyond

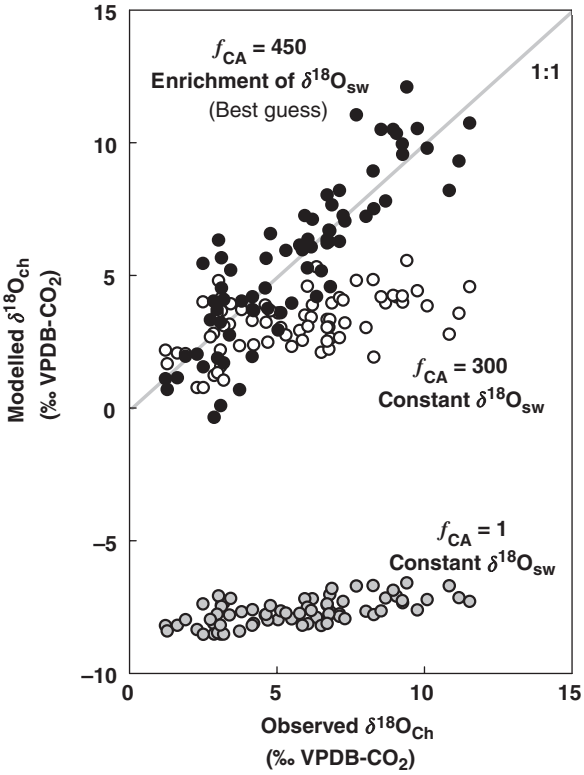

Fig. 10 Comparison of the observed and predicted oxygen isotope signatures of the net soil CO_2 flux in chambers 1 and 2 combined. The different symbols refer to different scenarios of hydration of CO_2 and surface soil $\delta^{18}O_{sw}$ (see the text for further details).

the scope of this particular field experiment. However, direct measurements of CA activity in soil surface layers are definitely required to confirm the results from our oxygen isotope studies of CO_2 fluxes from the field.

Our results also indicated that enhanced hydration was required in the uppermost soil layers (0–5 cm), where soil CO_2 concentrations were likely to have ranged from 0.05% to 0.4%, respectively. Such low concentrations (relative to those of the bulk soil concentrations) would increase the demand for CA activity in the anaplerotic processes detailed in Table 3. At ambient CO_2 levels, the growth of organisms depend on sufficient CA activity, and different types of CA are abundantly expressed (Kusian *et al*., 2002; Mitsuhashi *et al*., 2004; Mogensen *et al*., 2006). Furthermore, the maximum abundance of bacteria, fungi and protozoa has been found in the top 5 cm of the soil profile for Mediterranean loam (Fierer *et al*., 2003) and other soils (Ekelund *et al*., 2001; Taylor *et al*., 2002). Resource availability such as C and N is likely to form the primary control of this pattern in soil microbial communities (Fierer *et al*., 2003).

The above pathways could also be extremely important in maintaining the function of microbial populations in such Mediterranean soil surfaces, exposed to prolonged periods of drought interspersed with rain pulse events. For instance, at low soil water potentials, bacteria and fungi accumulate cytoplasmic solutes, primarily low molecular weight carbohydrates, polyols, amino acids, and amines, to lower intracellular water potentials and maintain cell turgor (Csonka & Hanson, 1991; Potts, 1994). Rapid increases in water potential can induce microbial cell lysis unless intracellular water potentials are immediately raised by some mechanism. One such mechanism is the release of these cytoplasmic solutes into the surrounding environment (Halverson *et al*., 2000; Sleator & Hill, 2001). A number of studies have shown that the accumulation of the osmoregulatory solutes in bacteria (primarily free amino acids, cf., Harris, 1981; Wood *et al*., 2001) is rapid and can represent between 10% and 20% of total cellular C in response to osmotic stress (Koujima *et al*., 1978). Such rapid accumulation of intracellular amino acids (including the glutamate family of amino acids and pyrimidines) would place a high demand on intermediates from the TCA cycle in order to construct carbon skeletons that would be generated from the products of glycolysis using PC (pyruvate carboxylase) or PEPc (phosphoenolpyruvate carboxylase) both requiring HCO_3^- and the expression of CA (Table 3). Therefore, we hypothesize that CA performs many essential roles in microbial DIC transport for surviving periods of osmotic stress, such as drought at the surface of Mediterranean soils. In addition, the release of such compatible solutes accompanied by rapid growth in microbial populations is thought to be at least partly responsible for the large pulses of CO_2 known as the Birch effect (Birch, 1958a, b) observed at the soil and ecosystem scale during and after rain pulses (Jarvis *et al*., 2007). The re-assimilation of this ephemerally available pool of C and N from the soil would also require the pathways of PC and/or PEPc (Table 3) to be active with potentially high CA expression in order for populations to grow quickly and capitalize on the transiently available resources.

Importance of near-surface isotopic enrichment in $\delta^{18}O_{sw}$

Efforts to monitor $\delta^{18}O_{sw}$ in ecosystems across the world at a monthly timescale are now in place (IAEA Moisture Isotopes in the Biosphere and Atmosphere; Hemming *et al*., 2007). These efforts will provide the information necessary to explore the effects of soil carbon and water cycling on $\delta^{18}O_a$ at the global scale. At present, the recommended protocol for measuring $\delta^{18}O_{sw}$ is to collect soil samples at a depth of 10 cm.

Table 3 Metabolic reactions in algae, bacteria, fungi and roots demanding inorganic C

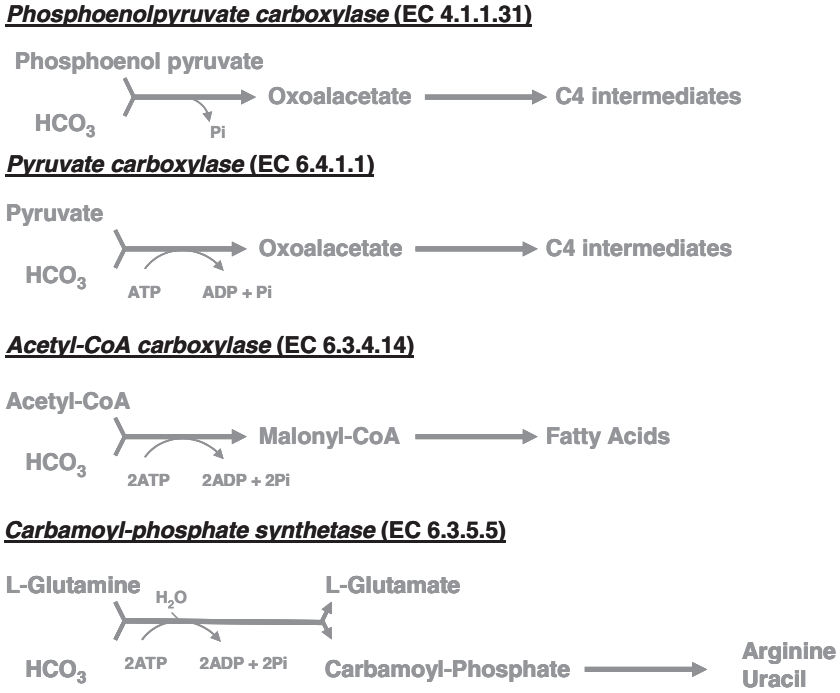

However, Melayah *et al*. (1996b) observed $\delta^{18}O_{sw}$ enrichments up to 17‰ (from −7‰ to + 10‰ VSMOW) in the top 10 cm of a bare clay loam soil profile. Depth-resolved values of $\delta^{18}O_{sw}$ are important for predicting $\delta^{18}O$ of soil CO_2 fluxes (Riley, 2005). In addition, soil profiles of $\delta^{18}O_{sw}$ can reflect the propagation of rain events down through the soil profile (Barnes & Allison, 1983, 1988). It is difficult to obtain such fine resolution information on $\delta^{18}O_{sw}$, particularly because $\delta^{18}O_{sw}$ data always reflects a combination of temporal and spatial variability of $\delta^{18}O_{sw}$ in the field. Instead, we will have to rely on numerical models to describe the transient evolution of the $\delta^{18}O$ of soil water (Melayah *et al*., 1996a) and soil CO_2 fluxes in response to environmental drivers.

Because our soil samples integrated $\delta^{18}O_{sw}$ over 5 cm depth, we may have underestimated the real value of $\delta^{18}O_{sw}$ at the soil surface. For this reason, we tested whether our observations could be explained by stronger enrichment of $\delta^{18}O_{sw}$ at the soil surface alone, without invoking a need for an enhanced rate of CO_2 hydration. We found that, to match the field data, we needed unrealistic $\delta^{18}O_{sw}$ at the soil surface between + 30‰ VSMOW at the beginning of the experiment and + 50‰ VSMOW at the end (Fig. 9; Scenario 2). Furthermore, an increase in the $\delta^{18}O_{sw}$ alone fails to capture the finer features of the data on the sub-diurnal timescale (Fig. 9). Including enhanced f_{CA} shows that these primarily result from interactions between the flux signatures in chambers ($\delta^{18}O_{ch}$) and the ambient CO_2 signatures ($\delta^{18}O_a \approx \delta^{18}O_i$). This was also found by Seibt *et al*. (2006) where diurnal variations in CO_2 fluxes, environmental drivers and soil water were extremely conservative, yet large diurnal variation in $\delta^{18}O_{ch}$ persisted mainly because of changes in $\delta^{18}O_a$. The isotope effects of changes in soil fluxes, leading to shifts in the balance between the net flux and the invasion flux, were typically small as were the temperature effects.

Lastly, it is unclear whether extracellular CA activity (for example, as in aquatic algae) accelerates the equilibration of soil CO_2 with water in soil pore spaces, or whether CO_2 equilibrates with intracellular water pools containing CA. If the isotopic exchange occurs within microbes, it may be important to consider offsets in $\delta^{18}O_{sw}$ between extra- and intracellular water. Recent laboratory studies on *Escherichia coli* indicate that the isotope composition of intracellular water can in fact be very different from extracellular water (Kreuzer-Martin *et al*., 2005, 2006). During active growth, most of the intracellular water (about 70%) was derived from metabolism. Further studies on this interesting topic are obviously required in the future to establish the impact of such metabolic activity on $\delta^{18}O_s$.

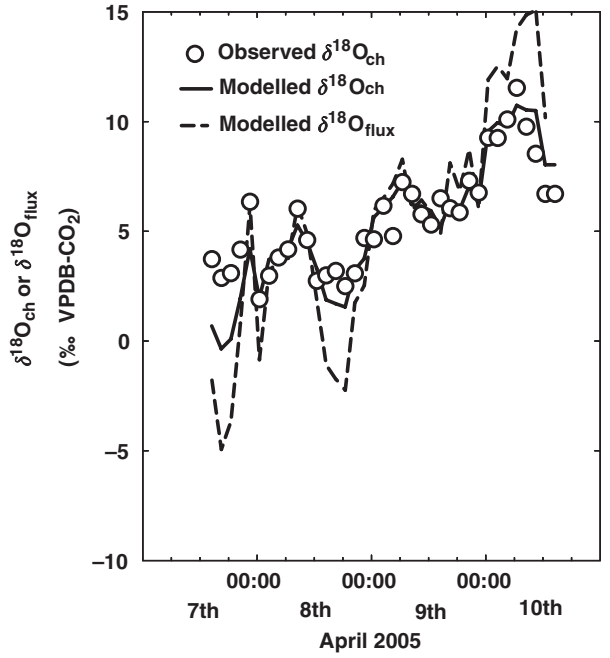

Fig. 11 Time series of the observed and predicted oxygen isotope signatures of the net soil CO_2 flux ($\delta^{18}O_{Ch}$) in chamber 2 (open circles) and the predicted oxygen isotope signatures of the net soil CO_2 flux.

Impact of our results for partitioning studies

The oxygen isotope composition of water in soils and leaves is often very different. For instance, the globally averaged isotopic composition of leaf water is + 5‰ VSMOW, while soil water has a global average value of −7‰ VSMOW (Keeling, 1993). It is this strong disequilibrium that lends itself well to $C^{18}O^{16}O$ partitioning studies at both the ecosystem (Langendörfer *et al*., 2002; Ogée *et al*., 2004) and global scales (Peylin *et al*., 1999). At the ecosystem scale, this tracer has the potential to help us retrieve not only photosynthesis and respiration (Ogée *et al*., 2004) but also the contribution of soil- and foliage-respired CO_2 fluxes to the total rate of nocturnal ecosystem respiration (Mortazavi & Chanton, 2002; Bowling *et al*., 2003).

A large isotopic disequilibrium between the $\delta^{18}O$ signals of photosynthesis and respiration is necessary for robust partitioning (Ogée *et al*., 2004). However, our results [and those of Seibt *et al*. (2006)] indicate that oxygen isotope signals of soil CO_2 fluxes can be affected by enhanced hydration, that may significantly change the outcome of partitioning studies.

Furthermore, our results illustrate that chamber measurements alone ($\delta^{18}O_{ch}$) cannot be used as a direct proxy for $\delta^{18}O_{flux}$, the signal required for partitioning studies. This is highlighted in Fig. 11, where we plot our best guess modelled values of $\delta^{18}O_{ch}$ and $\delta^{18}O_{flux}$ alongside the observed $\delta^{18}O_{ch}$ (see also Figs 2 and 3). The $\delta^{18}O_{ch}$ and $\delta^{18}O_{flux}$ signatures can differ substantially (up to ± 5‰). Because of the finite chamber air volume, a larger fraction of chamber CO_2 is in equilibrium with soil water, such that over time, $\delta^{18}O_{flux}$ signals are no longer fully expressed i.e. chambers tend to dampen the extremes, both negative and positive (see also Seibt *et al*., 2006). Thus, $\delta^{18}O_{sw}$ changes affect $\delta^{18}O_{ch}$ less than $\delta^{18}O_{flux}$. The extent of divergence between $\delta^{18}O_{flux}$ and $\delta^{18}O_{ch}$ depends on the relative strength of the invasion, increasing with CA and at lower net flux rates. A soil diffusion model that takes these effects into account is required to interpret chamber observations.

Although the theory of $CO^{18}O$ transport in soils is well developed (Hesterberg & Siegenthaler, 1991; Amundson *et al*., 1998; Tans, 1998), all partitioning studies so far have used a simpler model to predict $\delta^{18}O_{flux}$, neglecting the invasion flux and assuming full equilibration with soil water: $\delta^{18}O_{flux} \approx \delta^{18}O_{eq} + \varepsilon_d$. Our data demonstrates that $\delta^{18}O_{flux}$ is not accurately predicted with such a simple equation. Indeed a full equilibration with the range of $\delta^{18}O_{sw}$ measured between 5 and 10 cm depth (−3‰ to 0‰ VSMOW) would result in $\delta^{18}O_{flux}$ values of about −10.5‰ to −6‰ VPDB-CO_2, while our data suggest much more enriched values (see Fig. 11). From our findings, it seems that a complete mechanistic model of the $\delta^{18}O$ of soil CO_2 fluxes (including possible enzymatic effects in soils) is necessary for estimating $\delta^{18}O_{flux}$. More studies linking experimental data and modelling in contrasting biomes are necessary before we are able to assess the degree of model complexity required to robustly describe the magnitude and phasing of oxygen isotope signals of CO_2 exchanged between soils and the atmosphere at larger scales. Our study certainly indicates that gradients of $\delta^{18}O_{sw}$ at the soil surface are not modelled with sufficient detail at the global scale yet to predict $\delta^{18}O_{flux}$. For instance, the recent global ^{18}O study of Cuntz *et al*. (2003a) relies on a simple soil 'bucket' model to predict $\delta^{18}O_{sw}$. As a result it has a tendency to underestimate the influence of soil evaporation on the seasonal variations of $\delta^{18}O_{sw}$, and thus $\delta^{18}O_{flux}$ (Cuntz *et al*., 2003a). However, it remains unclear whether an improved modelling approach for soil water isotopes, atmospheric transport of CO_2 and/or 'biological' processes in the soil will account for the current inability of global models to reproduce the seasonal phasing of the atmospheric oxygen isotope signal for almost all flask network stations (Peylin *et al*., 1999; Cuntz *et al*., 2003b). Moreover, it is still too early to predict how CA activity varies spatially or temporally. This will only be resolved with further field and laboratory investigations. When studies can provide

constraints on the level of activity expected for this enzyme in different soils, then we can begin to explore how sensitive the response of the atmospheric oxygen isotope signal is to this additional biological mechanism.

Conclusions

We found that the oxygen isotope composition of net CO_2 fluxes from drying Mediterranean soils was dynamic over diurnal and daily timescales. Our results indicate that short periods (a few days) of hot dry weather after small rain events enrich the oxygen isotope composition of water pools at the soil surface and transfer this isotopic enrichment to $C^{18}O^{16}O$ in the atmosphere. Our study also highlights that assuming a constant relationship between $\delta^{18}O_{sw}$ and CO_2 concentration is not appropriate for predicting soil flux $\delta^{18}O$ signatures, especially when CA is present. Only when we included an enhanced CO_2 hydration and isotopic equilibration term (mediated by the presence of CA) and an evaporative enrichment term of $\delta^{18}O_{sw}$ at the soil surface could we match the observations. We discussed a number of processes requiring CA which are necessary for soil microbes and fine roots to grow and function at the CO_2 concentrations found close to the soil surface. Measuring fine-scale variations in the oxygen isotope composition of soil water ($\delta^{18}O_{sw}$) in the field is extremely difficult, but detailed modelling and field validation of soil water dynamics (and CA activity) can help to interpret the data. These tests are also crucial before we can use the oxygen isotopes of CO_2 to partition gross photosynthesis and respiration at larger scales.

Acknowledgements

We thank Raquel Lobo de Vale, Cathy Besson, Stephan Unger, Joao Banza and Alan Pike for assistance in the field. We also thank Manuela Negreanu for the IRMS work, Prof. John Raven FRS, Bill Riley, Joe Berry and Jon Massheder for their helpful and encouraging discussions.

This study was made possible through the EU-funded projects – Mediterranean IN Drought (MIND Project No. – EVK2-CT-2002-00158) to M. M., a Carboeurope-IP grant awarded to Professor John Grace FRSE, University of Edinburgh and a Marie Curie International Fellowship awarded to Ulli Seibt (MOIF-CT-2004-2704).

References

Aguilera J, van Dijken JP, de Winde JH, Pronk JT (2005) Carbonic anhydrase (Nce103p): an essential biosynthetic enzyme for growth of *Saccharomyces cerevisiae* at atmospheric carbon dioxide pressure. *Biochemistry Journal*, **391**, 311–316.

Amoroso G, Morell-Avrahov L, Muller D, Klug K, Sultemeyer D (2005) The gene NCE103 (YNL036w) from *Saccharomyces cerevisiae* encodes a functional carbonic anhydrase and its transcription is regulated by the concentration of inorganic carbon in the medium. *Molecular Microbiology*, **56**, 549–558.

Amundson R, Stern L, Baisden T, Wang Y (1998) The isotopic composition of soil and soil-respired CO_2. *Geoderma*, **82**, 83–114.

Barnes CJ, Allison GB (1983) The distribution of deuterium and ^{18}O in dry soils 1. Theory. *Journal of Hydrology*, **60**, 141–156.

Barnes CJ, Allison GB (1988) Tracing of water movement in the unsaturated zone using stable isotopes of hydrogen and oxygen. *Journal of Hydrology*, **100**, 143–176.

Birch HF (1958a) Further aspects of humus decomposition. *Nature*, **182**, 1172.

Birch HF (1958b) Pattern of humus decomposition in East African soils. *Nature*, **181**, 788.

Bird R, Stewart W, Lightfoot E (2002) *Transport Phenomena*. John Wiley, Hoboken, NJ.

Bowling DR, McDowell NG, Welker JM, Bond BJ, Law BE, Ehleringer JR (2003) Oxygen isotope content of CO_2 in nocturnal ecosystem respiration: 2. Short-term dynamics of foliar and soil component fluxes in an old-growth ponderosa pine forest. *Global Biogeochemical Cycles*, **17**, 1124, doi: 10.1029/2003GB002082.

Brenninkmeijer CAM, Kraft P, Mook WG (1983) Oxygen isotope fractionation between CO_2 and H_2O. *Isotope Geoscience*, **1**, 181–190.

Brown OR, Howitt HF (1969) Growth inhibition and death of *Escherichia coli* from CO_2 deprivation. *Microbios*, **3**, 241–246.

Chang K, Roberts JKM (1992) Quantitation of rates of transport, metabolic fluxes, and cytoplasmic levels of inorganic carbon in maize root tips during K^+ ion uptake. *Plant Physiology*, **99**, 291–297.

Conrad R (1996) Soil microorganisms as controllers of atmospheric trace gases (H_2, CO, CH_4, OCS, N_2O and NO). *Microbiological Reviews*, **60**, 609–640.

Csonka L, Hanson A (1991) Prokaryotic osmoregulation: genetics and physiology. *Annual Review of Microbiology*, **45**, 569–606.

Cubash U, von Storch H, Waskewitz J, Zorita E (1996) Estimates of climate change in Southern Europe derived from dynamical climate model output. *Climate Research*, **7**, 129–149.

Cuntz M, Ciais P, Hoffmann G, Knorr W (2003a) A comprehensive global three-dimensional model of $\delta^{18}O$ in atmospheric CO_2: 1. Validation of surface processes. *Journal of Geophysical Research*, **108**, 4527, doi: 10.1029/2002JD003153.

Cuntz M, Ciais P, Hoffmann G, Knorr W (2003b) A comprehensive global three-dimensional model of $\delta^{18}O$ in atmospheric CO_2: 2. Mapping the atmospheric signal. *Journal of Geophysical Research*, **108**, 4528, doi: 10.1029/2002JD003154.

David TS (2000) *Intercepcao da precipitacao e transpiracao em arvores isoladas de Q. rotundifolia Lam*. Universidade Tecnia de Lisboa, Lisboa, Portugal, 155 pp.

Dehority BA (1971) Carbon dioxide requirement of various species of rumen bacteria. *Journal of Bacteriology*, **105**, 70–76.

Ekelund F, Ronn R, Christensen S (2001) Distribution with depth of protozoa, bacteria and fungi in soil profiles from three Danish forest sites. *Soil Biology and Biochemistry*, **33**, 475–481.

Farquhar GD, Lloyd J, Taylor JA *et al*. (1993) Vegetation effects on the isotope composition of oxygen in atmospheric CO_2. *Nature*, **363**, 439–443.

Fierer N, Schimel JP, Holden PA (2003) Variations in microbial community composition through two soil depth profiles. *Soil Biology and Biochemistry*, **35**, 167–176.

Gutknecht J, Bisson MA, Tosteson FC (1977) Diffusion of carbon dioxide through lipid bilayer membranes – effects of carbonic anhydrase, bicarbonate and unstirred layers. *The Journal of General Physiology*, **69**, 779–794.

Halverson LJ, Jones TM, Firestone MK (2000) Release of intracellular solutes by four soil bacteria exposed to dilution stress. *Soil Science Society of America Journal*, **64**, 1630–1637.

Harris R (1981) *Effect of water potential on microbial growth and activity*. Water Potential Relations in Soil Microbiology. SSSA Spec. Pub. 9, Madison, pp. 23–95.

Hemming D, Loader N, Marca A, Robertson I, Williams D, Wingate L, Yakir D (2007) The future of large-scale stable isotope networks. In: *Stable Isotopes as Indicators of Ecological Change. Terrestrial Ecology Series* (eds Dawson T, Siegwolf R), pp. 361–381. Elsevier, Academic Press, Amsterdam.

Hemming D, Yakir D, Ambus P *et al*. (2005) Pan-European $\delta^{13}C$ values of air and organic matter from forest ecosystems. *Global Change Biology*, **11**, 1065–1093.

Hesterberg R, Siegenthaler U (1991) Production and stable isotopic composition of CO_2 in a soil near Bern, Switzerland. *Tellus*, **43B**, 197–205.

Jarvis PG, Rey A, Petsikos C *et al*. (2007) Drying and wetting of Mediterranean soils stimulates decomposition and carbon dioxide emission: the ''birch effect''. *Tree Physiology*, **27**, 929–940.

Kapiluto Y, Yakir D, Tans PP, Berkowitz B (2007) Experimental and numerical studies of the ^{18}O exchange between CO_2 and water in the atmosphere-soil invasion flux. *Geochemica et Cosmochimica Acta*, **71**, 2657–2671.

Keeling RF (1993) Heavy carbon dioxide. *Nature*, **363**, 399.

Kesselmeier J, Hubert A (2002) Exchange of reduced volatile sulfur compounds between leaf litter and the atmosphere. *Atmospheric Environment*, **36**, 4679–4686.

Kesselmeier J, Teusch N, Kuhn U (1999) Controlling variables for the uptake of atmospheric carbonyl sulfide by soil. *Journal of Geophysical Research*, **104**, 11577–11584.

Klengel T, Liang WJ, Chaloupka J *et al*. (2005) Fungal adenylyl cyclase integrates CO_2 sensing with cAMP signalling and virulence. *Current Biology*, **15**, 2021–2026.

Koujima I, Hayashi H, Tomochika K, Okabe A, Kanemasa Y (1978) Adaptational change in proline and water content of *Staphylococcus aureus* after alteration of environmental salt concentration. *Applied Environmental Microbiology*, **35**, 467–470.

Kozliak EI, Guilloton MB, Fuchs JA, Anderson PM (2000) Bacterial carbonic anhydrases. In: *The Carbonic Anhydrases: New Horizons* (eds Chegwidden WR, Carter ND, Edwards YH), pp. 547–565. Birkhauser, Basel, Switzerland.

Kreuzer-Martin HW, Ehleringer JR, Hegg EL (2005) Oxygen isotopes indicate most intracellular water in log-phase *Escherichia coli* is derived from metabolism. *Proceedings of the National Academy of Sciences of the United States of America*, **102**, 17337–17341.

Kreuzer-Martin HW, Lott MJ, Ehleringer JR, Hegg EL (2006) Metabolic processes account for the majority of the intracellular water in log-phase *Escherichia coli* cells as revealed by hydrogen isotopes. *Biochemistry*, **45**, 13622–13630.

Kuhn U, Ammann C, Wolf A, Meixner FX, Andreae MO, Kesselmeier J (1999) Carbonyl sulfide exchange on an ecosystem scale: soil represents a dominant sink for atmospheric COS. *Atmospheric Environment*, **33**, 995–1008.

Kurz-Besson C, Otieno D, Lobo do Vale R *et al*. (2006) Hydraulic lift in cork oak trees in a savannah-type Mediterranean ecosystem and its contribution to the local water balance. *Plant and Soil*, **282**, 361–378.

Kusian B, Sultemeyer D, Bowien B (2002) Carbonic anhydrase is essential for growth of *Ralstonia eutropha* at ambient CO_2 concentrations. *Journal of Bacteriology*, **184**, 5018–5026.

Langendörfer U, Cuntz M, Ciais P *et al*. (2002) Modelling of biospheric CO_2 gross fluxes via oxygen isotopes in a spruce forest canopy: a ^{222}Rn calibrated box model approach. *Tellus*, **54B**, 476–496.

Lavorel S, Canadell J, Rambal S, Terradas J (1998) Mediterranean terrestrial ecosystems: research priorities on global change effects. *Global Ecology and Biogeography Letters*, **7**, 157–166.

Li W, Yu L, He Q *et al*. (2005) Effects of microbes and their carbonic anhydrase on Ca^{2+} and Mg^{2+} migration in column-built leached soil–limestone karst systems. *Applied Soil Ecology*, **29**, 274–281.

Li W, Yu L, Yuan D *et al*. (2004) Bacteria biomass and carbonic anhydrase activity in some karst areas of Southwest China. *Journal of Asian Earth Sciences*, **24**, 145–152.

Melayah A, Bruckler L, Bariac T (1996a) Modeling the transport of water stable isotopes in unsaturated soils under natural conditions. 1. Theory. *Water Resources Research*, **32**, 2047–2054.

Melayah A, Bruckler L, Bariac T (1996b) Modeling the transport of water stable isotopes in unsaturated soils under natural conditions. 2. Comparison with field experiments. *Water Resources Research*, **32**, 2055–2065.

Miller JB, Yakir D, White JWC, Tans PP (1999) Measurement of $^{18}O/^{16}O$ in the soil-atmosphere CO_2 flux. *Global Biogeochemical Cycles*, **13**, 761–774.

Miranda P, Coelho FES, Tome AR, Valente MA (2002) Twentieth century portuguese climate and climate scenarios. In: *Climate Change in Portugal. Scenarios, Impacts and Adaptation Measures – SIAM Project* (eds Santos FD, Forbes K, Moita R), pp. 25–83. Gradiva, Lisbon.

Mitsuhashi S, Ohnishi J, Hayashi M, Ikeda M (2004) A gene homologous to β-type carbonic anhydrase is essential for the growth of *Corynebacterium glutamicum* under atmospheric conditions. *Applied Microbiology and Biotechnology*, **63**, 592–601.

Mogensen EG, Janbon G, Chaloupka J *et al*. (2006) *Cryptococcus neoformans* senses CO_2 through the carbonic anhydrase Can2 and the adenylyl cyclase Cac1. *Eukaryotic Cell*, **5**, 103–111.

Moldrup P, Olesen T, Yamaguchi T, Schjonning P, Rolston DE (2003) Modeling diffusion and reaction in soils: X. A unifying model for solute and gas diffusivity in unsaturated soil. *Soil Science*, **168**, 321–337.

Mortazavi B, Chanton JP (2002) Carbon isotopic discrimination and control of nighttime canopy $\delta^{18}O$-CO_2 in a pine forest in the southeastern United States. *Global Biogeochemical Cycles*, **16**, 1008, doi: 10.1029/2000GB001390.

Ogée J, Peylin P, Cuntz M *et al*. (2004) Partitioning net ecosystem carbon exchange into net assimilation and respiration with canopy-scale isotopic measurements: an error propogation

analysis with $^{13}CO_2$ and $CO^{18}O$ data. *Global Biogeochemical Cycles*, **18**, GB2019, doi: 10.1029/2003GB002166.

Pereira JS, Mateus JA, Aires LM *et al*. (2007) Effects of drought – altered seasonality and low rainfall – in net ecosystem carbon exchange of three contrasting Mediterranean ecosystems. *Biogeosciences Discussions*, **4**, 1703–1736.

Peylin P, Ciais P, Denning AS *et al*. (1999) A 3-dimensional study of $\delta^{18}O$ in atmospheric CO_2: contribution of different land ecosystems. *Tellus Series B – Chemical and Physical Meteorology*, **51**, 642–667.

Potts M (1994) Dessication tolerance of prokaryotes. *Microbiological Reviews*, **58**, 755–805.

Press WH, Flannery BP, Teukolsky SA, Vetterling WT (1989) *Numerical Recipes: FORTRAN*. Cambridge University Press, New York.

Raven JA, Newman JR (1994) Requirement for carbonic anhydrase activity in processes other than photosynthetic inorganic carbon assimilation. *Plant, Cell & Environment*, **17**, 123–130.

Rayment M, Jarvis PG (1997) An improved open chamber system for measuring soil CO_2 effluxes in the field. *Journal of Geophysical Research*, **102**, 28779–28784.

Riley WJ (2005) A modeling study of the impact of the $\delta^{18}O$ value of near-surface soil water on the $\delta^{18}O$ value of the soil-surface CO_2 flux. *Geochemica et Cosmochimica Acta*, **69**, 1939–1946.

Riley WJ, Still CJ, Helliker BR, Ribas-Carbo M, Berry JA (2003) ^{18}O composition of CO_2 and H_2O ecosystem pools and fluxes in a tallgrass prairie: simulations and comparisons to measurements. *Global Change Biology*, **9**, 1567–1581.

Riley WJ, Still CJ, Torn MS, Berry JA (2002) A mechanistic model of $H_2^{18}O$ and $C^{18}OO$ fluxes between ecosystems and the atmosphere: model description and sensitivity analyses. *Global Biogeochemical Cycles*, **4**, 1095, doi: 10.1029/2002GB001878.

Seibt U, Wingate L, Lloyd J, Berry JA (2006) Diurnally variable $\delta^{18}O$ signatures of soil CO_2 fluxes indicate carbonic anhydrase activity in a forest soil. *Journal of Geophysical Research*, **111**, G04005, doi: 10.1029/2006JG000177.

Simmons JS, Klemedtsson L, Hultberg H, Hines ME (1999) Consumption of atmospheric carbonyl sulfide by coniferous boreal forest soils. *Journal of Geophysical Research*, **104**, 11569–11576.

Sleator R, Hill C (2001) Bacterial osmoadaptation: the role of osmolytes in bacterial stress and virulence. *FEMS Microbiological Reviews*, **25**, 49–71.

Steinbacher M, Bingemer HG, Schmidt U (2004) Measurements of the exchange of carbonyl sulfide (OCS) and carbon disulfide (CS_2) between soil and atmosphere in a spruce forest in central Germany. *Atmospheric Environment*, **2004**, 6043–6052.

Tans PP (1998) Oxygen isotopic equilibrium between carbon dioxide and water in soils. *Tellus*, 163–178.

Taylor JP, Wilson B, Mills MS, Burns RG (2002) Comparison of microbial numbers and enzymatic activities in surface soils and subsoils using various techniques. *Soil Biology and Biochemistry*, **34**, 387–401.

Van Diest H, Kesselmeier J (2007) Soil atmosphere exchange of carbonyl sulfide (COS) regulated by diffusivity depending on water-filled pore space. *Biogeosciences Discussions*, **4**, 3701–3722.

Viktor A, Cramer MD (2005) The influence of root assimilated inorganic carbon on nitrogen acquisition/assimilation and carbon partitioning. *New Phytologist*, **165**, 157–169.

Wood JM, Bremer E, Csonka LN, Kraemer R, Poolman B, van der Heide T, Smith LT (2001) Osmosensing and osmoregulatory compatible solute accumulation by bacteria. *Comparative Biochemistry and Physiology*, **130A**, 437–460.

Yakir D, Wang XF (1996) Fluxes of CO_2 and water between terrestrial vegetation and the atmosphere estimated from isotope measurements. *Nature*, **380**, 515–517.

Appendix A

The model setup consisted of 21 layers of increasing thickness down to 1 m depth, ranging from 1-cm-thick layers at the top of the profile to 10-cm-thick layers near the bottom (between 40 and 100 cm depth). Model simulations were performed for each chamber measurement using profile data on soil temperature and volumetric water content concurrently collected at the field site. The soil CO_2 production profile was parameterized using root biomass data presented in Kurz-Besson *et al*. (2006), either including or excluding the large roots. The two profiles gave almost identical predictions (not shown).

The model was run until the soil profiles of CO_2 and $C^{18}O^{16}O$ reached a steady state. Then, the infinite air space above the soil was replaced by the (virtual) soil chamber, and the model run continued over the duration of the measurement, [i.e. chamber closure period of 15 min (Fig. 3)]. Equations (2) and (4) were solved using the implicit differencing method (Press *et al*., 1989). We used a time step of 10^{-3} s for the transient calculations over chamber closure periods. From the gradients of CO_2 and $C^{18}O^{16}O$ at the soil surface, we then calculated the $\delta^{18}O$ signatures of the net soil CO_2 fluxes at each time step. To obtain model results directly comparable to the observations, we also calculated 'modelled chamber' signatures from the same simple mass balance [Eqn (1)] as used for the field data.

